

# Localized states in the continuum in low-dimensional systems

Khee-Kyun Voo\* and C. S. Chu

*Department of Electrophysics, National Chiao Tung University, Hsinchu 30010, Taiwan, Republic of China*

(Dated: August 27, 2018)

It is shown in this paper that for open systems, states which are localized in space, discrete in energy, and embedded in the continuum of extended states, can be sustained by low-dimensional and channeled leads. These states have an origin different from that of analogous states discussed by J. von Neumann and E. Wigner [Phys. Z. **30**, 465 (1929)]. A few representative systems are discussed. These states cause, for example, infinitely sharp Fano resonance in transport when they are marginally destroyed.

PACS numbers: 73.22.Dj, 03.65.Ge, 73.23.Ad, 73.63.-b

## I. INTRODUCTION

Shortly after the discovery of quantum mechanics, von Neumann and Wigner pointed<sup>1,2</sup> out that potentials defining closed boundary conditions were not the only cause of discrete and localized (normalizable) states. They pointed out that localized states could also be due to the destructive interference in the Bragg scattering from certain long-ranged wiggling potentials defining open boundary conditions. These states are embedded in the continuum, decay in space with a power dependence, and have been studied in atomic and molecular systems<sup>2,3,4</sup> and superlattices.<sup>5</sup> In this paper, we show that analogous states can also be found in open systems with low-dimensional leads. They decay exponentially in space in contrast to those discussed by von Neumann and Wigner,<sup>1,2</sup> and also have a different origin. Moreover, they are shown to be related to the infinitely sharp Fano resonance<sup>6</sup> in transport.

To illustrate the properties of such states in low-dimensional systems, three representative model systems will be discussed — A tight-binding (TB) molecular system, a quantum graph with doubly-connected one-dimensional (1D) channels, and a waveguide in a two-dimensional (2D) space. All three are open systems. The first two are simple enough for analytic analyses, where some generic properties can be studied rigorously. The third one is to illustrate the presence of these states in more realistic systems, but unfortunately, it allows only a numerical analysis.

## II. MODELS AND DISCUSSIONS

### A. A tight-binding molecular system

First we consider the TB system shown in Fig. 1(a) which is defined by the Hamiltonian

$$H = H_{\text{mol}} + H_{\text{lead}} + H_{\text{mol-lead}},$$

$$H_{\text{mol}} \equiv \sum_{i=1}^4 c_i^\dagger V_i c_i + \sum_{i=1}^4 \sum_{j>i} [c_i^\dagger h_{ij} c_j + \text{H.c.}],$$

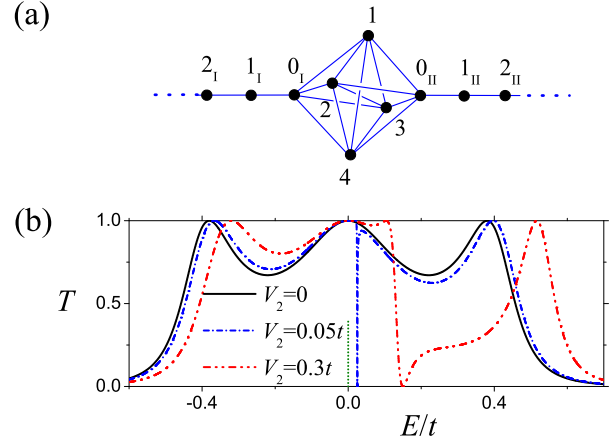


FIG. 1: (Color online) (a) The considered open TB system, which consists of a molecule with four sites (labeled by 1 ~ 4) connected to two leads (labeled by I and II) with serially connected sites (labeled by  $i_\eta$  for lead  $\eta$ , where  $i = 0 \sim \infty$  and  $\eta = \text{I and II}$ ). The hoppings are denoted by bonds. (b) The transmission probability  $T$  at different energies for  $V_2 = 0$  (solid line), where there is a LSC (located by a dotted line); and  $V_2 = 0.05t$  (dash-dotted line) and  $0.3t$  (dash-dot-dotted line), where there are no LSC. Those not-mentioned system parameters are referred to the text.

$$H_{\text{lead}} \equiv -t \sum_{\eta=\text{I,II}} \sum_{i=0}^{\infty} c_{(i+1)_\eta}^\dagger c_{i_\eta} + \text{H.c.},$$

$$H_{\text{mol-lead}} \equiv \sum_{\eta=\text{I,II}} \sum_{i=1}^4 c_{0_\eta}^\dagger h_{0_\eta i} c_i + \text{H.c.}, \quad (1)$$

where  $c_\lambda$ ,  $\lambda \in \{1 \sim 4, 0_{\text{I}} \sim \infty_{\text{I}}, 0_{\text{II}} \sim \infty_{\text{II}}\}$ , is the annihilation operator of a spinless particle on site  $\lambda$ ,  $t$  and  $V_i$  are real, and  $h_{ij}$  and  $h_{0_\eta i}$  are complex in general. Sites 1 ~ 4 are in a “molecule”, and sites  $0_\eta \sim \infty_\eta$  are in lead  $\eta$ ,  $\eta = \text{I and II}$ . This Hamiltonian may describe a nanoscopic molecule or a mesoscopic cluster of quantum dots connected to two leads.

Using a basis set  $\{|\lambda\rangle\}$  defined by  $|\lambda\rangle \equiv c_\lambda^\dagger |0\rangle$

and  $c_\lambda|0\rangle \equiv 0$ , one can write the time-independent Schrödinger equation (TISE)  $H|\psi\rangle = E|\psi\rangle$ , where  $E$  is the energy of the particle, into a set of simultaneous finite-difference (FD) equations. In a lead, the FD equations read  $t\psi_{j-1}^\eta + E\psi_j^\eta + t\psi_{j+1}^\eta = 0$ , for  $j = 1 \sim \infty$  and  $\eta = \text{I or II}$ , where  $\psi_j^\eta \equiv \langle j_\eta|\psi\rangle$ . It has an analytic solution

$$\psi_j^\eta = A_\eta e^{-ikj} + B_\eta e^{ikj}, \quad (2)$$

where  $A_\eta$  and  $B_\eta$  are arbitrary complex numbers, and  $k \equiv |k| \equiv \cos^{-1}[-E/(2t)] \equiv k(E)$ . Since  $k > 0$ , the ingoing or inward propagating wave amplitudes are  $A_\text{I}$  and  $A_\text{II}$ .

There remains six FD equations not solved by Eq. (2). Replacing  $\psi_0^\eta$  and  $\psi_1^\eta$  by  $A_\eta$  and  $B_\eta$  using Eq. (2), and writing  $\psi_j \equiv \langle j|\psi\rangle$  for  $j = 1 \sim 4$ , the six equations can be written as a matrix equation,

$$\begin{bmatrix} -te^{ik(E)} - E & h_{0\text{I}1} & h_{0\text{I}2} & h_{0\text{I}3} & h_{0\text{I}4} & 0 \\ h_{0\text{I}1}^* & V_1 - E & h_{12} & h_{13} & h_{14} & h_{0\text{II}1}^* \\ h_{0\text{I}2}^* & h_{12}^* & V_2 - E & h_{23} & h_{24} & h_{0\text{II}2}^* \\ h_{0\text{I}3}^* & h_{13}^* & h_{23}^* & V_3 - E & h_{34} & h_{0\text{II}3}^* \\ h_{0\text{I}4}^* & h_{14}^* & h_{24}^* & h_{34}^* & V_4 - E & h_{0\text{II}4}^* \\ 0 & h_{0\text{II}1} & h_{0\text{II}2} & h_{0\text{II}3} & h_{0\text{II}4} & -te^{ik(E)} - E \end{bmatrix} \begin{bmatrix} B_\text{I} \\ \psi_1 \\ \psi_2 \\ \psi_3 \\ \psi_4 \\ B_\text{II} \end{bmatrix} = \begin{bmatrix} (E + te^{-ik(E)}) A_\text{I} \\ -h_{0\text{I}1}^* A_\text{I} - h_{0\text{II}1}^* A_\text{II} \\ -h_{0\text{I}2}^* A_\text{I} - h_{0\text{II}2}^* A_\text{II} \\ -h_{0\text{I}3}^* A_\text{I} - h_{0\text{II}3}^* A_\text{II} \\ -h_{0\text{I}4}^* A_\text{I} - h_{0\text{II}4}^* A_\text{II} \\ (E + te^{-ik(E)}) A_\text{II} \end{bmatrix}, \quad (3)$$

where the components from top to bottom are respectively the FD equations centered at sites  $0_\text{I}$ , 1, 2, 3, 4, and  $0_\text{II}$ . When  $A_\text{I}$  and  $A_\text{II}$  are given, there are six unknowns ( $B_\text{I}$ ,  $\psi_1$ ,  $\psi_2$ ,  $\psi_3$ ,  $\psi_4$ , and  $B_\text{II}$ ) to be found. The unknowns can be found by a straightforward matrix inversion when the square matrix has a nonzero determinant. Notably, the determinant actually can *vanish* at certain energies for some system configurations, and imply a nontrivial solution at  $A_\text{I} = A_\text{II} = 0$  (no ingoing waves). The solution must be localized within the molecule, since the outgoing wave amplitudes  $B_\text{I}$  and  $B_\text{II}$  are necessarily vanishing due to unitarity.

The determinant of the square matrix in Eq. (3) vanishes whenever the rows or columns of the matrix are not linearly independent. For instance, consider the config-

uration  $h_{0\text{I}2} = h_{0\text{I}3}$ ,  $h_{0\text{II}2} = h_{0\text{II}3}$ ,  $h_{12} = h_{13}$ ,  $h_{24} = h_{34}$ ,  $h_{23} = h_{23}^*$ , and  $V_2 = V_3$ , at the energy  $E = V_2 - h_{23}$ . In this occasion, the third and fourth rows of the matrix are seen to be identical, which means that the determinant of the matrix vanishes, and the solution to the problem is not unique. Note that the system in this configuration is not really “symmetric” in the usual sense.

A complete solution  $\Psi(\lambda)$  for Eq. (3), in the case of a simple symmetric system in which  $h_{12} = h_{13} = h_{24} = h_{34} \equiv \Delta$ ,  $h_{0\text{I}1} = h_{0\text{II}4} \equiv \Gamma$ , and  $h_{14} = h_{23} = h_{0\text{I}2} = h_{0\text{I}3} = h_{0\text{I}4} = h_{0\text{II}1} = h_{0\text{II}2} = h_{0\text{II}3} = V_1 = V_2 = V_3 = V_4 = 0$  (which is similar to the model considered in Ref. 7), at  $E = 0$  (i.e.,  $k = \pi/2$ ), where the determinant vanishes, is found to be

$$\begin{aligned} \Psi(\lambda) &= \psi_{\text{ext}}(\lambda) + \beta\psi_{\text{loc}}(\lambda), \\ \psi_{\text{ext}}(\lambda) &= \frac{t(A_\text{I} - A_\text{II})}{i\Gamma}(\Delta_{\lambda,1} - \Delta_{\lambda,4}) - \frac{\Gamma}{\Delta}(A_\text{I}\Delta_{\lambda,2} + A_\text{II}\Delta_{\lambda,3}) \\ &\quad + \sum_{j=0}^{\infty} [(i^{-j}A_\text{I} + i^jA_\text{II})\Delta_{\lambda,j\text{I}} + (i^{-j}A_\text{II} + i^jA_\text{I})\Delta_{\lambda,j\text{II}}], \\ \psi_{\text{loc}}(\lambda) &= \Delta_{\lambda,2} - \Delta_{\lambda,3}, \end{aligned} \quad (4)$$

where  $\beta$  is an arbitrary complex number,  $i \equiv \sqrt{-1}$ , and  $\Delta_{\lambda,\lambda'} = 1$  (0) when  $\lambda = \lambda'$  ( $\lambda \neq \lambda'$ ).  $\Psi$  is seen to be a superposition of an extended state  $\psi_{\text{ext}}$  and a localized state  $\psi_{\text{loc}}$ . When  $A_\text{I} = A_\text{II} = 0$  or  $|\beta| \rightarrow \infty$ ,  $\Psi \rightarrow \psi_{\text{loc}}$  and it is a localized state in the continuum (LSC).

The origin of the LSCs in TB systems can also be

understood in a more direct manner, given an insight from the observation that  $\psi_{\text{loc}}$  vanishes at the sites in the molecule in contact with the leads [see Eq. (4)]. In general, if  $\psi_A$  and  $\psi_B$  are respectively the stationary states at an energy  $E$  in two isolated clusters of sites, labeled by  $A$  and  $B$ , and  $\psi_A(j_A^0) = \psi_B(j_B^0) = 0$ , where  $j_A^0$  ( $j_B^0$ ) is

a site on cluster  $A$  ( $B$ ), then the direct product  $\psi_A \otimes \psi_B$  is a stationary state at  $E$  in a system where clusters  $A$  and  $B$  are coupled by  $t_{AB}c_{j_A^0}^\dagger c_{j_B^0} + \text{H.c.}$  This is because though the FD equations for the coupled clusters contain the additional terms  $t_{AB}\psi(j_B^0)$  and  $t_{AB}^*\psi(j_A^0)$ , the wave function  $\psi_A \otimes \psi_B$  is still a solution of the FD equations since these terms vanish due to  $\psi_A(j_A^0) = \psi_B(j_B^0) = 0$ . If one of the clusters, say cluster  $A$ , is infinitely large or open and  $\psi_A$  is trivial, whereas cluster  $B$  is finite sized and  $\psi_B$  is nontrivial, then  $\psi_A \otimes \psi_B$  is a LSC. The generalization of the above argument to the case with more than two clusters is straightforward. An example of such case is the LSC in Eq. (4), which can be constructed from three clusters, where two of them (the two leads) have infinitely large sizes and trivial stationary states.

For  $A_I = 1$  and  $A_{II} = 0$ , the transmission probability  $T$  defined by  $T \equiv |B_{II}|^2$  is plotted versus the energy  $E$  for  $\Delta = 0.2t$  and  $\Gamma = 0.4t$  in Fig. 1(b). In the same figure,  $T$  is also plotted for the same system parameters but  $V_2 = 0.05t$  and  $0.3t$ , where the LSC is destroyed and has become an almost-localized state. It is seen that  $T$  can reflect the LSC only when the LSC is destroyed by a perturbation and a Fano resonance appears.<sup>8</sup> The blue shifts of the resonances from the energy of the LSC is due to the increase of the energies of the almost-localized states by  $V_2$ .

Therefore a comprehensive understanding of the problem may be stated as the following. For problems of open systems, whenever the determinant of the matrix to be inverted vanishes at an energy, there is a localized state at that energy. If the energy is in a continuum of extended scattering states, the localized state is a LSC, and a complete solution is a superposition of the degenerate LSC and extended states. As the states are decoupled, the transport which is related only to the extended states does not reflect the presence of the LSC. When a LSC is destroyed, or a previously localized state is coupled with the extended states, the passing of a particle from one

lead to the other through the molecule can take place via two routes — the extended states spanning the leads and the molecule or the almost-localized state in the molecule. That results in a nonresonant and a resonant transmission amplitudes, and the interference results in a Fano resonance.<sup>6</sup> When the almost-localized state is on the verge of the decoupling from the continuum and acquiring an infinitely long lifetime, the resonance is infinitely sharp.<sup>9</sup>

## B. A quantum graph

The second example is a quantum graph. The quantum graphs are multiply-connected 1D systems, which are meant to be effective models of multiply-connected quasi-one-dimensional (Q1D) systems at low energies. They are defined by the following conditions. Away from the junctions, a particle is governed by a 1D Schrödinger equation. At a junction, the wave functions on different branches are connected by a chosen connecting scheme.<sup>10</sup> For a junction of three branches, we have chosen a scheme defined by the equations (1)  $\psi_1 = \psi_2 = \psi_3$  and (2)  $\nu\psi_1 + \sum_{i=1}^3 \partial\psi_i/\partial x_i = 0$ , where  $\psi_i$  and  $x_i$  are respectively the wave function and coordinate defined on branch  $i$ . The coordinates are directed away from the junction, and  $\nu$  is a given real parameter with a dimension of 1/length.

We consider a 1D ring connected to two 1D leads as shown in Fig. 2(a). A potential everywhere equal to zero is assumed, and the wave function at energy  $E$  on the branch labeled by  $\eta$  ( $\eta = \text{I, II, III, and IV}$ ) is  $\psi^\eta(x_\eta) = A_\eta e^{ikx_\eta} + B_\eta e^{-ikx_\eta}$ , where  $A_\eta$  and  $B_\eta$  are arbitrary complex numbers and  $k \equiv \sqrt{2mE}/\hbar$ . Applying the mentioned connecting scheme at the two junctions, we obtain six simultaneous equations or a matrix equation,

$$\begin{bmatrix} -1 & 1 & 1 & 0 & 0 & 0 \\ -1 & 0 & 0 & 1 & 1 & 0 \\ 1 - i\nu/k & 1 & -1 & 1 & -1 & 0 \\ 0 & e^{ikL_{II}} & e^{-ikL_{II}} & 0 & 0 & -1 \\ 0 & 0 & 0 & e^{ikL_{III}} & e^{-ikL_{III}} & -1 \\ 0 & -e^{ikL_{II}} & e^{-ikL_{II}} & -e^{ikL_{III}} & e^{-ikL_{III}} & 1 - i\nu/k \end{bmatrix} \begin{bmatrix} B_I \\ A_{II} \\ B_{II} \\ A_{III} \\ B_{III} \\ B_{IV} \end{bmatrix} = \begin{bmatrix} A_I \\ A_I \\ A_I(1 - i\nu/k) \\ A_{IV} \\ A_{IV} \\ A_{IV}(1 - i\nu/k) \end{bmatrix}, \quad (5)$$

where  $L_{II}$  and  $L_{III}$  are respectively the lengths of branches II and III. When the ingoing wave amplitudes  $A_I$  and  $A_{IV}$  are specified, there are six unknowns to be found ( $B_I$ ,  $A_{II}$ ,  $B_{II}$ ,  $A_{III}$ ,  $B_{III}$ , and  $B_{IV}$ ).

From Eq. (5), a LSC is seen at  $k = k_n \equiv nn_0\pi/L_0$ , when  $L_{II} : L_{III} = n_{II} : n_{III}$ ,  $n_0 \equiv \min(n_{II}, n_{III})$ ,

$L_0 \equiv \min(L_{II}, L_{III})$ ,  $n$ ,  $n_{II}$ , and  $n_{III}$  are integers, and  $n_{II} + n_{III}$  is even. The above condition results in  $e^{ik_n L_{II}} = e^{ik_n L_{III}} = (-1)^{nn_0} \equiv \zeta_n$ , and for the square matrix in Eq. (5), the differences between the corresponding elements in the first and second rows are identical to that between the fourth and fifth rows. Therefore the

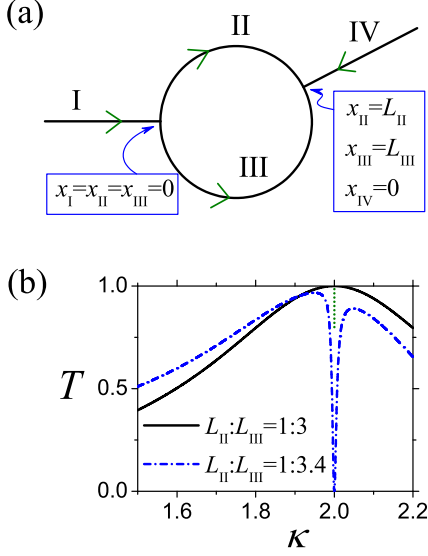


FIG. 2: (Color online) (a) The considered open quantum graph, which consists of a 1D ring (formed by the branches labeled by II and III) connected to two leads (labeled by I and IV). A coordinate  $x_\eta$  with a positive direction indicated by an arrow is defined on branch  $\eta$  ( $\eta = I, II, III$ , and IV). (b) The transmission probability  $T$  is plotted versus a dimensionless wave number  $\kappa$  defined by  $\kappa \equiv k(L_{II} + L_{III})/(2\pi)$ , for  $\nu = 0$ , and  $L_{II} : L_{III} = 1 : 3$  (solid line) and  $1 : 3.4$  (dash-dotted line). There is a LSC for the  $1 : 3$  case (indicated by a dotted line), but not for the  $1 : 3.4$  case in this energy range.

$$\begin{aligned}
 \Psi_n(x) &= \psi_n^{\text{ext}}(x) + \beta \psi_n^{\text{loc}}(x), \\
 \psi_n^{\text{ext}}(x) &= \sum_{\eta=I,IV} [A_\eta e^{ik_n x_\eta} + \Lambda_n(\bar{A}_\eta, A_\eta) e^{-ik_n x_\eta}] \Delta_{x,x_\eta} \\
 &\quad + \sum_{\eta=II,III} [\Omega_n(A_I, A_{IV}) e^{ik_n x_\eta} + \Omega_n(A_{IV}, A_I) e^{ik_n(L_\eta - x_\eta)}] \Delta_{x,x_\eta}, \\
 \psi_n^{\text{loc}}(x) &= \sin(k_n x_{II}) \Delta_{x,x_{II}} - \sin(k_n x_{III}) \Delta_{x,x_{III}}, \\
 \Lambda_n(X, Y) &\equiv \frac{\zeta_n X - Y \nu_n}{1 + \nu_n}, \quad \Omega_n(X, Y) \equiv \frac{X(3 + \nu_n) + \zeta_n Y(1 - \nu_n)}{4(1 + \nu_n)}, \\
 \bar{A}_I &\equiv A_{IV}, \quad \bar{A}_{IV} \equiv A_I, \\
 \nu_n &\equiv \frac{\nu}{ik_n},
 \end{aligned} \tag{6}$$

where  $\beta$  is an arbitrary complex number, and  $\Delta_{x,x_\eta} = 1$  (0) when  $x = x_\eta$  ( $x \neq x_\eta$ ). The solution  $\Psi_n$  is a superposition of a LSC  $\psi_n^{\text{loc}}$  and an extended state  $\psi_n^{\text{ext}}$ . Like in the case of a TB model discussed in Sec. II A,  $\psi_n^{\text{loc}}$  vanishes at the point in contact with the leads

Since the LSC is decoupled from the extended states, it will not be revealed in those spectral properties due to the scattering. For quantum graphs, Texier<sup>11</sup> has pointed

rows are not linearly independent and the determinant of the matrix vanishes. A complete solution  $\Psi_n(x)$ , where  $x \in \{x_\eta \mid \eta = I, II, III, IV\}$ , is found to be

out that the Friedel sum rule, which is related to the phases of the eigenvalues of the scattering matrix, fails to count the number of states in a scattering region in such a situation. Experimentally, it has also been found<sup>12</sup> that a 1D lead does not couple to a 2D wave function when the lead is located at a node of the wave functions.

The LSCs in the defined quantum graph can also be understood directly from the connecting equations at

the junctions. If a stationary state at energy  $E$  in a graph labeled by  $A$ , has a node at a point  $P$  on one of the branches, then labeling the segments of the branch on the two sides of  $P$  by 1 and 2, defining coordinates  $x_1$  and  $x_2$  respectively, with positive directions directed away from  $P$ , and denoting the stationary wave functions on segments 1 and 2 by  $\psi_1(x_1)$  and  $\psi_2(x_2)$  respectively, one has  $\psi_1 = \psi_2$  (both are vanishing) and  $\partial\psi_1/\partial x_1 + \partial\psi_2/\partial x_2 = 0$  at  $P$ , and the stationary wave function can be written in the form of the direct product  $\psi_1 \otimes \psi_2 \otimes \psi_{\text{others}}^A$ , where  $\psi_{\text{others}}^A$  is the direct product of the wave functions on the other branches in the graph. Similarly, for a graph labeled by  $B$  containing a branch with an open end labeled by 3, which has also a stationary state at  $E$ , the stationary wave function can be written into the form  $\psi_3 \otimes \psi_{\text{others}}^B$ , where  $\psi_3$  is the wave function on branch 3, and  $\psi_{\text{others}}^B$  is the direct product of the wave functions on the other branches in the graph. If  $\psi_3$  is trivial, when the open end of branch 3 is attached to  $P$  by demanding the connecting equations  $\psi_1 = \psi_2 = \psi_3$  and  $\nu\psi_1 + \sum_{i=1}^3 \partial\psi_i/\partial x_i = 0$  to be fulfilled at  $P$ , the direct product  $\psi_1 \otimes \psi_2 \otimes \psi_3 \otimes \psi_{\text{others}}^A \otimes \psi_{\text{others}}^B$  is a stationary solution at  $E$  in the coupled graphs, since the connecting equations are automatically fulfilled. If graph  $A$  is finite and  $\psi_1 \otimes \psi_2 \otimes \psi_{\text{others}}^A$  is nontrivial, whereas graph  $B$  is infinitely large and  $\psi_3 \otimes \psi_{\text{others}}^B$  is trivial, the stationary state in the coupled graphs is a LSC. Note that the above arguments can also be straightforwardly generalized to the case of more than two clusters, and the LSC in Eq. (6) is an example of this.

For  $A_I = 1$  and  $A_{IV} = 0$ , the transmission probability  $T$  defined by  $T = |B_{IV}|^2$ . In Fig. 2(b),  $T$  is plotted versus the wave number for  $\nu = 0$ ,  $L_{II} : L_{III} = 1 : 3$  and  $1 : 3.4$ , at the vicinity of a LSC or almost-localized state. For an isolated ring with a uniform potential on it, the nodes of the stationary standing wave states are equally spaced, and hence ‘‘commensurate’’ branch lengths (such as 1:3) in the open graph give rise to LSCs. Note the Fano resonance when the LSC is destroyed.

### C. A two-dimensional waveguide

Our third example is a waveguide in a 2D continuous space as shown in Fig. 3(a). The waveguide has a width of  $W$ , and the potential in the waveguide is set at zero besides a square region that is set at  $V_G$ . We will call the infinitely extended regions on both sides the leads, and the central finite sized region a resonating cavity. This system may model a mesoscopic fabricated structure.

We discretize the continuous space into a square lattice, and the TISE becomes a set of simultaneous FD equations that read<sup>13,14</sup>  $-t(\psi_{\mathbf{i}-\hat{x}} + \psi_{\mathbf{i}+\hat{x}} + \psi_{\mathbf{i}-\hat{y}} + \psi_{\mathbf{i}+\hat{y}}) + (V_{\mathbf{i}} - E + 2t)\psi_{\mathbf{i}} = 0$ , where  $E$  is the energy,  $t \equiv \hbar^2/(2ma^2)$  ( $a$  is the distance between two nearest sites),  $\hat{x}$  and  $\hat{y}$  are respectively the unit vectors along the  $x$  and  $y$  directions,  $\mathbf{i} \equiv (i_x, i_y)$  (where  $i_x$  and  $i_y$  are integers), and  $\psi_{\mathbf{i}}$  and  $V_{\mathbf{i}}$

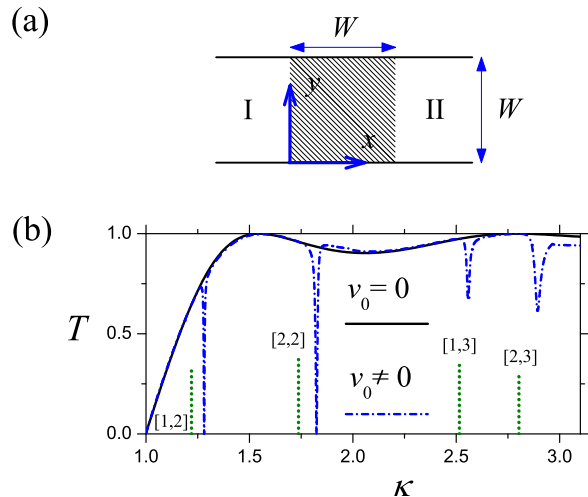


FIG. 3: (Color online) (a) The considered open 2D waveguide. Two leads (labeled by I and II) of width  $W$  are attached oppositely to a square cavity (shaded region). The potential in the leads are kept at zero, and that in the cavity is kept at  $V_G$ . A coordinate system  $(x, y)$  is defined in the cavity as shown. (b) The transmission probability  $T$  is plotted versus a dimensionless wave number  $\kappa$  defined by  $\kappa \equiv \sqrt{2mEW}/(\pi\hbar)$ , for the case shown in (a) (solid line) and the case with an additional  $\delta$ -potential  $V(x, y) = v_0\delta(x - W/6)\delta(y - W/6)$  (dashed-dotted line). In this energy range, LSCs (indicated by dotted lines) are found only in the case of no  $\delta$ -potential. The pairs of integers in the form  $[m_x, m_y]$  indicate the profiles of the LSCs.

are respectively the wave function and potential at  $\mathbf{i}a$ . The FD equations are solved like in the first example.

In a lead labeled by  $\eta$  ( $\eta = I$  or  $II$ ), taking the integer  $i_x^\eta$  ( $i_y^\eta$ ) as the longitudinal (transverse) coordinate, the wave function at energy  $E$  for  $V_{\mathbf{i}} = 0$  is<sup>13,14</sup>

$$\psi^\eta(i_x^\eta, i_y^\eta) = \sum_{m=1}^{N_\eta} \left( A_m^\eta e^{ik_m^\eta i_x^\eta a} + B_m^\eta e^{-ik_m^\eta i_x^\eta a} \right) \times \frac{1}{\sqrt{N_\eta + 1}} \sin \left[ \frac{m\pi}{N_\eta + 1} (i_y^\eta + 1) \right], \quad (7)$$

where  $A_m^\eta$  and  $B_m^\eta$  are arbitrary complex numbers,  $i_y^\eta = 0 \sim N_\eta - 1$  [where  $W \equiv (N_\eta + 1)a$ ], and  $k_m^\eta$  is defined by  $E \equiv -2t\{2 - \cos(k_m^\eta a) - \cos[m\pi/(N_\eta + 1)]\}$ , where the cosine is defined by  $\cos \xi \equiv (e^{i\xi} + e^{-i\xi})/2$  for a complex  $\xi$ , and the phase of  $k_m^\eta$  is chosen such that  $A_m^\eta$  is the amplitude of a wave propagating or exponentially decaying inward. The multiple transverse modes for the transverse coordinate  $i_y^\eta$  is a consequence of the quasi-one-dimensionality.

Taking the ingoing amplitudes  $\{A_m^\eta\}$  as the input, the unknowns will be  $\{B_m^\eta\}$  (amplitudes of the waves propagating or exponentially decaying outward) and the pointwise wave function in the cavity  $\psi_{\text{cavity}}$ . The FD equations centered at the sites within the cavity, and the

uniqueness requirement of the wave function at the interfaces between the cavity and the leads results in a matrix equation of the form

$$M(E) \cdot \{|B_m^\eta\rangle, \psi_{\text{cavity}}\} = \{|A_m^\eta\rangle\}, \quad (8)$$

where  $\{|A_m^\eta\rangle\}$  and  $\{|B_m^\eta\rangle, \psi_{\text{cavity}}\}$  are respectively the known and unknown column matrices, and  $M(E)$  is a square matrix whose determinant  $\det M(E)$  may vanish and imply LSCs in the system.

When there are no ingoing waves (i.e.,  $A_m^\eta = 0$  for all  $\eta$  and  $m$ ) and hence  $\{|A_m^\eta\rangle\} = 0$ , a nontrivial solution for  $\{|B_m^\eta\rangle, \psi_{\text{cavity}}\}$  can be obtained if  $\det M(E) = 0$ . This is necessarily a localized state since the  $B_m^\eta$ 's for the outward propagating waves necessarily vanish due to unitarity, leaving only the possibility of nonvanishing  $B_m^\eta$ 's for the outward exponentially decaying waves. If  $\det M(E) = 0$  occurs at an energy  $E_0$  in the continuum, a complete solution at  $E_0$  is a superposition of the localized state found by  $\det M(E) = 0$ , and the extended states found by inverting  $M(E)$  at  $E_0 + \delta$ ,  $\delta \rightarrow 0$ .

Note that to find a nontrivial solution for the column vector  $|\phi\rangle$  in an equation  $S|\phi\rangle = 0$ , where  $S$  is a square matrix, is to find an eigenvector of  $S$  that corresponds to a vanishing eigenvalue (since the equation is just  $S|\phi\rangle = 0 \cdot |\phi\rangle$ ). The eigenproblem can be solved by a numerical package such as EISPACK (<http://www.netlib.org/>). In general, there can be simultaneously more than one eigenvectors having vanishing eigenvalues, and these eigenvectors are the degenerate localized states in the original problem.

Figure 3(b) shows the transmission probability  $T$  for a particle with an energy  $E$ , injected from the first subband in lead I, and passed to the first subband in lead II. Letting  $A_m^\eta = \Delta_{\eta,1} \Delta_{m,1}$ ,  $T$  is given by  $T \equiv |B_1^{II}|^2$ . We choose  $V_G = -15\hbar^2/(mW^2)$ , and consider the cases with and without an additional perturbing  $\delta$ -potential  $V(x, y) = v_0\delta(x - W/6)\delta(y - W/6)$  in the cavity,<sup>15</sup> where  $v_0 = 5\hbar^2/m$ , and  $x$  and  $y$  are the coordinates defined in Fig. 3(a).

In the considered energy range in Fig. 3(b), zeroes of  $\det M(E)$ <sup>16</sup> or LSCs are found only for the case without a perturbing  $\delta$ -potential. Note that LSCs can also exist at energies beyond the first subband (at  $\kappa > 2$ ). We have used  $N_\eta = 17$  in Fig. 3(b), and since we find the LSCs qualitatively the same as those in the calculation using  $N_\eta = 8$ ,<sup>17</sup> we believe they will survive in the continuous space limit. As usual, Fano resonances appear when the LSCs are destroyed. The locations of the resonances depend on the details of the perturbing potential, but when the perturbing potentials are vanishingly small, the resonances are always found with infinitesimal widths on the locations of the LSCs. A noteworthy point is the  $\delta$ -potential does not affect a LSC when it is on a node of it.

The LSCs in Fig. 3(b) have profiles with exponential tails in the leads, and resemble the fictitious standing waves  $\sin(m_x\pi x/W) \cdot \sin(m_y\pi y/W)$  in the cavity,

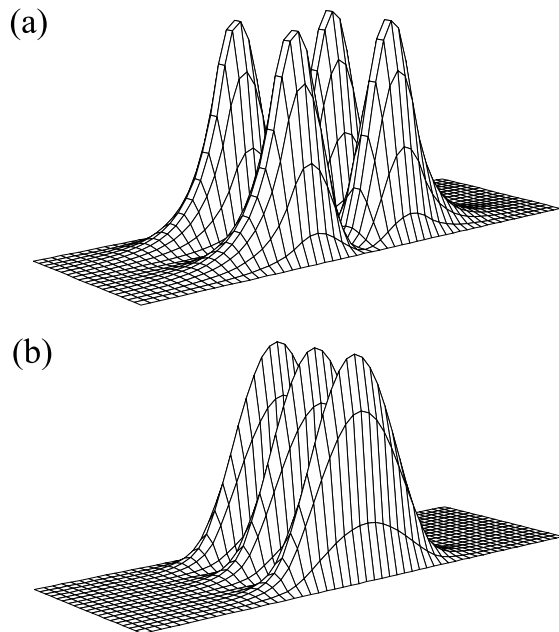


FIG. 4: The probability densities of two of the LSCs in Fig. 3(b) are shown in a section of the waveguide with the cavity at the center. The length of the section is three times of the width. (a) The [2,2] LSC at  $\kappa \simeq 1.74$  has sizable exponential tails in the leads. Correspondingly, it has also a considerable red shift from  $\kappa_{\text{SW}}(2, 2) \simeq 2.23$ , where  $\kappa_{\text{SW}}(m_x, m_y)$  is defined by  $\kappa_{\text{SW}}(m_x, m_y) \equiv \sqrt{2mE_{\text{SW}}(m_x, m_y)W}/(\pi\hbar)$ . (b) The [1,3] LSC at  $\kappa \simeq 2.51$  has smaller exponential tails in the leads, and also a lesser red shift from  $\kappa_{\text{SW}}(1, 3) \simeq 2.64$ .

where  $m_x$  and  $m_y$  are integers. Therefore we will use  $[m_x, m_y]$  to label the LSCs for the convenience in our discussion. The four LSCs in Fig. 3(b), from the lowest to the highest energy, resemble standing waves with  $[m_x, m_y] = [1, 2], [2, 2], [1, 3],$  and  $[2, 3]$  respectively. The probability densities or squares of the absolute values of the wave functions of two of the LSCs are shown in Fig. 4. The energy of a LSC is found to be always red shifted from the energy of the corresponding fictitious standing wave in the cavity  $E_{\text{SW}}(m_x, m_y)$ , where  $E_{\text{SW}}(m_x, m_y) = V_G + (m_x^2 + m_y^2)\pi^2\hbar^2/(2mW^2)$ . Moreover, it seems that the larger the exponential tails, the more the red shift [comparing Figs. 4(a) and 4(b)]. This is conceivable since the tails lead to a lowering of the kinetic energies.

The presence of the above LSCs can be understood by an intuitive picture. Notice that the first two LSCs which resemble the  $[m_x, m_y] = [1, 2]$  and  $[2, 2]$  standing waves, are embedded only in the first subband. Since their transverse wave functions resemble  $\sin(2\pi y/W)$  and are orthogonal to the first transverse modes in the leads  $\sin(\pi y/W)$ , the standing waves are trapped in the cavity. With this picture, the absence of a LSC with  $m_y = 1$ , such as a LSC with  $[m_x, m_y] = [2, 1]$  or  $[3, 1]$  is conceiv-

able. The two higher energy LSCs which resemble the standing waves with  $[m_x, m_y] = [1, 3]$  and  $[2, 3]$  are embedded in both the first and second subband. Likewise, the trapping can be understood by the observation that their transverse wave functions with  $m_y = 3$  are orthogonal to the transverse modes in the leads with  $m_y = 1$  and 2. In this energy range we do not find LSCs with  $m_y = 1$  and 2, such as  $[3, 1]$  and  $[3, 2]$ .<sup>18,19,20,21</sup>

The LSCs as the eigenstates of  $M(E)$  are orthogonal to each other, though the  $M(E)$  in Eq. (8) is non-Hermitian in general. The orthogonality can be argued from the fact that the LSCs are localized and are not affected by a truncation of the leads at distances far away from the cavity. Since the LSCs form a subset of the set of eigenenergy states of the Hermitian Hamiltonian matrix for the truncated (closed) system, they are orthogonal.

### III. CONCLUDING REMARKS

The behaviors of the LSCs in open low-dimensional systems have been illustrated by examples of various kinds. These LSCs are obtained by studying the zeroes of the determinant of the matrix to be inverted in a consid-

ered problem. A zero corresponds to at least one localized state. The crucial factor in the formation of these LSCs is the low-dimensionality of the leads, and the ‘‘symmetricity’’ in the systems is not a necessary condition.<sup>22</sup>

For the TB molecule and quantum graph, the one-dimensionality of the leads enables them to attach just at the nodes of a LSC in the scattering region and thereby leaving the LSC intact. The same argument also holds for the case of higher dimensional leads with 1D constrictions at the ends joining the scattering region. For the case of Q1D leads, the delocalization of a standing wave in the cavity can be prohibited by the non-overlapping of its transverse wave function and the transverse modes in the leads, and the standing wave is turned into a LSC.<sup>23</sup>

In view of the possibility of such LSCs not only in the case of idealized 1D leads but also in the case of Q1D leads, such LSCs may exist or may be realizable in, e.g., mesoscopic structures<sup>24</sup> and nanobridges or molecular junctions,<sup>25</sup> and may not of academic interest only.

**Acknowledgments** - This work is supported by the National Science Council of Taiwan under Grant No. 94-2112-M-009-017, and we also thank S.W. Chung for helpful discussions.

---

\* Corresponding author (Email: kkvoo@cc.nctu.edu.tw).

<sup>1</sup> J. von Neumann and E. Wigner, Phys. Z. **30**, 465 (1929).

<sup>2</sup> F. H. Stillinger and D. R. Herrick, Phys. Rev. A **11**, 446 (1975)

<sup>3</sup> H. Friedrich and D. Wintgen, Phys. Rev. A **31**, 3964 (1985).

<sup>4</sup> L. S. Cederbaum, R. S. Friedman, V. M. Ryaboy, and N. Moiseyev, Phys. Rev. Lett. **90**, 13001 (2003); and the references therein.

<sup>5</sup> F. Capasso, C. Sirtori, J. Faist, D. L. Sivco, S.-N. G. Chu, and A. Y. Cho, Nature **358**, 565 (1992); and the references therein.

<sup>6</sup> U. Fano, Nuovo cimento **12**, 156 (1935); Phys. Rev. **124**, 1866 (1961).

<sup>7</sup> Z. Y. Zeng, F. Claro, and A. Perez, Phys. Rev. B **65**, 85308 (2002).

<sup>8</sup> A numerical inversion blindly implemented by a computer on a matrix with a vanishing determinant can be stable. This may be due to the finite precision. For instance, a  $V_2 = 0$  calculation where the determinant can vanish, may be implemented as, say, a  $V_2 \sim 10^{-8}t$  calculation where the determinant does not vanish, and the resulting fake Fano resonance is too sharp to be noticeable.

<sup>9</sup> Such Fano resonance has been seen in the theoretical study of many systems (e.g., see Ref. 7), but an explicit solution in the form of Eq. 4 has not been reported.

<sup>10</sup> K.-K. Voo, S.-C. Chen, C.-S. Tang, and C.-S. Chu, Phys. Rev. B **73**, 35307 (2006); and the references therein.

<sup>11</sup> C. Texier, J. Phys. A **35**, 3389 (2002).

<sup>12</sup> J. Stein and H.-J. Stöckmann, Phys. Rev. Lett. **68**, 2867 (1992).

<sup>13</sup> S. Datta, *Electronic Transport in Mesoscopic Systems*, 1st

ed. (Cambridge University Press, Cambridge, 1995).

<sup>14</sup> D. K. Ferry and S. M. Goodnick, *Transport in Nanostructures*, 1st ed. (Cambridge University Press, Cambridge, 1997).

<sup>15</sup> A  $\delta$ -potential in a continuous space  $V_0 a^2 \delta(x - n_x a) \delta(y - n_y a)$  is modeled by a potential  $V_0 \Delta_{i_x, n_x} \Delta_{i_y, n_y}$  in the discretized space.

<sup>16</sup> Since  $\det M(E)$  is complex when  $E$  is in the continuum, a zero here means only a simultaneous vanishing of the real and imaginary parts within numerical precision. For Fig. 3(b), the precision is a width  $\delta\kappa < 10^{-3}$  on the  $\kappa$ -axis. By the same token, any structure in  $T$  sharper than  $\delta\kappa$  will not be seen.

<sup>17</sup> K.-K. Voo and C. S. Chu (unpublished).

<sup>18</sup> The understanding discussed in this paragraph may be related to the reports in Refs. 19,20,21.

<sup>19</sup> R. L. Schult, D. G. Ravenhall, and H. W. Wyld, Phys. Rev. B **39**, 5476 (1989).

<sup>20</sup> C. S. Kim, A. M. Satanin, Y. S. Joe, and R. M. Cosby, Phys. Rev. B **60**, 10962 (1999).

<sup>21</sup> A. F. Sadreev, E. N. Bulgakov, and I. Rotter, Phys. Rev. B **73**, 235342 (2006).

<sup>22</sup> A discussion of LSCs in asymmetric Q1D waveguides will be published elsewhere.

<sup>23</sup> Similar phenomena may also appear in other wave systems. Such as electromagnetic, acoustic, and water waves in waveguides, as the transverse confinements also lead to transverse modes.

<sup>24</sup> J. Göres, D. Goldhaber-Gordon, S. Heemeyer, M. A. Kastner, H. Shtrikman, D. Mahalu, and U. Meirav, Phys. Rev. B **62**, 2188 (2000); and the references therein.

<sup>25</sup> N. Sergeev, D. Roubtsov, and H. Guo, Phys. Rev. Lett.

95, 146803 (2005); and the references therein.